IRAQI JOURNAL OF MATERIALS
Volume (2) Issue (2) April-June 2023, pp. 75-82

Gas Sensing Characteristics of CuO-doped MgO Thin Films Prepared by Pulsed-Laser Deposition

Fuad T. Ibrahim

Department of Physics, College of Science, University of Baghdad, Baghdad, IRAQ

Abstract
In this work, pure and doped magnesium oxide (MgO) thin films doped with different concentrations (0.05, 0.07 and 0.1 wt.%) of copper oxide (CuO) were deposited on glass substrates by pulsed-laser deposition technique to fabricate gas sensors. The x-ray diffraction (XRD) patterns of prepared MgO:CuO nanostructures exhibit that the films are polycrystalline with tetragonal rutile phase for MgO and monoclinic phase for CuO. The transmittance and energy gap of all prepared samples were decreased while the absorption coefficient was increased with increasing CuO content. The effects of varying operation temperature of the fabricated gas sensors on sensor sensitivity and response time were studied. Maximum sensitivity of about 99.34% was determined for pure MgO.

Keywords: Gas sensing; Magnesium oxide; Copper oxide; Pulsed-laser deposition
Received: 22 November 2022; **Revised:** 27 January 2023; **Accepted:** 3 February; **Published:** 1 April 2023

1. Introduction

In the last years, nanoparticles of transition conducting metal oxides (TCMOs) were intensively investigated. The structural and optical properties of these TCMO nanoparticles are of particular interest [1-4]. In technological applications, oxides are used in the fabrication of microelectronic circuits, sensors, fuel cells and as catalysts [5-7]. In the emerging field of nanotechnology, a goal is to make nanostructures or nanoarrays with special properties with respect to those of bulk or single particle species [8]. The TCMO nanoparticles can exhibit inimitable physical and chemical properties due to their limited sizes and high density of corner or edge surface sites [9]. Recently, the II-VI semiconductor nanocrystals are developed as a class of nanomaterials whose unique physical and chemical properties are helping to create a new generation of nano-photonics, nano-optoelectronics and nano-electronics [10-12].

The catalytic behavior of metal oxides may be described in the reaction involving oxidation process [13]. The catalytic system of oxide-type catalysts is of particular importance where the active component exists in different oxidation states [14,15]. The catalytic activity of oxide catalysts is controlled by sites present in small concentration on its surface. Some metal oxides are very sensitive to the method of preparation and activation conditions. One of these oxides is copper oxide (CuO) [16].

In this work, fabrication of $(MgO)_{1-x}(CuO)_x$ thin films at room temperature on glass substrates by pulsed-laser deposition technique with different concentrations of CuO is aimed. The effects of CuO content on structural, optical and gas sensing properties are studied.

2. Experimental work

Highly pure (99.99%) powders of magnesium oxide (MgO) and copper oxide (CuO) supplied by Nanoshell Co. were mixed at different concentrations of CuO (0, 0.05, 0.07 and 0.1 wt.%) using gate mortar for one hour. The mixture was pressed under 5 tons pressure using SPECAC hydraulic piston for 10 minutes to form pellets of 1 cm in diameter and 0.2 cm in thickness. These pellets were sintered

 ISSN (print) 2958-8960 (online) xxxx-xxxx Printed in IRAQ

in air to temperature of 500 °C for 3 hours then cooled down to room temperature. The sintering temperature of the furnace was increased at a rate of 10 °C/min.

The substrates were cleaned with distilled water in order to remove any impurities then with alcohol and ultrasonic waves for 15 minutes to remove contaminants such as grease and some oxides. They were dried by blowing air and wiped with soft paper.

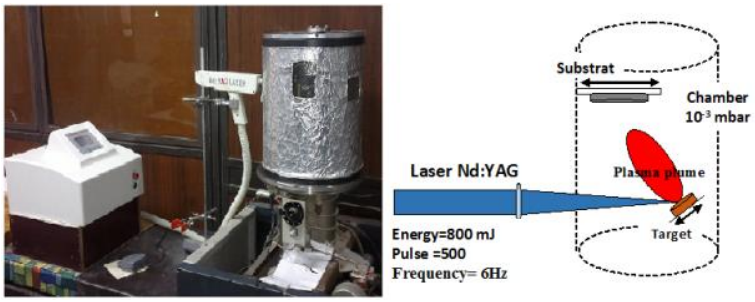

Fig. (1) The experimental setup of PLD used in this work

The pulsed-laser deposition (PLD) experiments were carried out inside a chamber evacuated down to 10^{-3} mbar. The target was irradiated by frequency-doubled Nd:YAG laser beam at 45° with the plane of target surface. This laser can deliver 800 mJ pulses with 9 ns pulse width and 6 Hz repetition rate. The maximum number of laser pulses used for irradiation was 500 pulses. The distance from the laser source to the target was set to 10 cm, and from the target to the substrate to 1.5 cm. Figure (1) shows the experimental setup used in this work.

A double-beam METERTECH SP8001 UV/VISIBLE spectrophotometer was used to measure the spectroscopic characteristics of the prepared samples in the spectral range of 320-1100nm. For the purpose of accuracy, the background correction was taken for each scan.

Aluminum electrodes were deposited on the surface of the prepared samples by thermal evaporation. The prepared samples were tested as gas sensors and figure (2) shows a schematic diagram of the experimental setup used for gas sensing measurements.

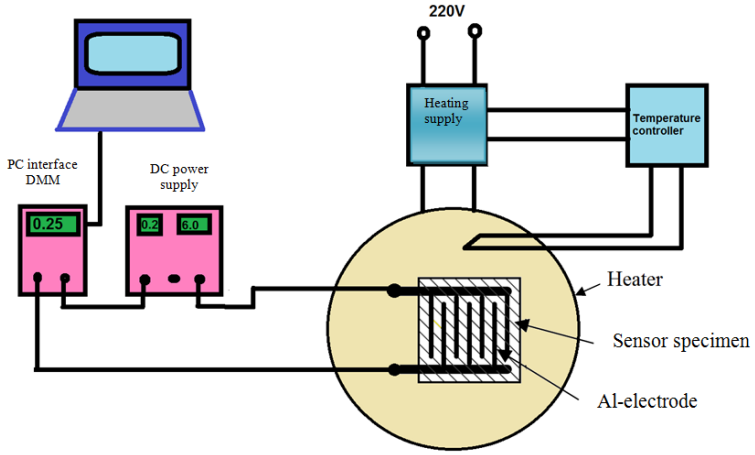

Fig. (2) Schematic diagram of gas sensing measurements and the required electrical circuit

3. Results and Discussion

The crystalline structure of $(MgO)_{1-x}(CuO)_x$ samples was recognized by the x-ray diffraction (XRD) patterns. Figure (3) shows these patterns for $(MgO)_{1-x}(CuO)_x$ thin films deposited on glass substrates at room temperature with 200 nm thickness at different concentrations of CuO (x= 0, 0.05, 0.07 and 0.1 wt.%). According to the International Center for Diffraction Data (ICDD), the structure of the deposited MgO films showed that they were polycrystalline tetragonal of rutile phase classification. The analysis verifies the reflection surfaces (110) and (021) for MgO [17] and (111), (022) and (202) for CuO [8]. When the concentration of CuO was increased, three peaks corresponding to reflection from (021), (022) and (202) planes were observed.

According to the results obtained from Hall Effect measurements shown in table (1), the pure and CuO-doped MgO films were p-type as the Hall voltage decreases with increasing the current. By using

ISSN (print) 2958-8960 (online) xxxx-xxxx Printed in IRAQ

the slope of this relationship, Hall coefficient (R_H), charge carrier and mobility were calculated. Table (2) shows the results of measured carrier concentration and type of conductivity of the prepared samples.

Figure (4) shows the UV-visible transmission spectra for the samples prepared at different concentrations of CuO in the wavelength range of 320-1100nm. It is clear that the transmittance is decreasing with increasing CuO concentration. It can be also observed that the peak of transmittance is decreased and shifted towards longer wavelengths with increasing CuO concentration [18]. This decrease in transmittance can be ascribed to the increase in the absorption induced by increasing CuO concentration in the final product. The shift in transmittance toward longer wavelength (i.e., lower energies) can be explained by increasing CuO content leading to increase the density of localized states and consequently the sample became much more opaque to the incident light. This causes the absorption edge to shift towards lower energies and hence the optical energy gap to shift towards lower values.

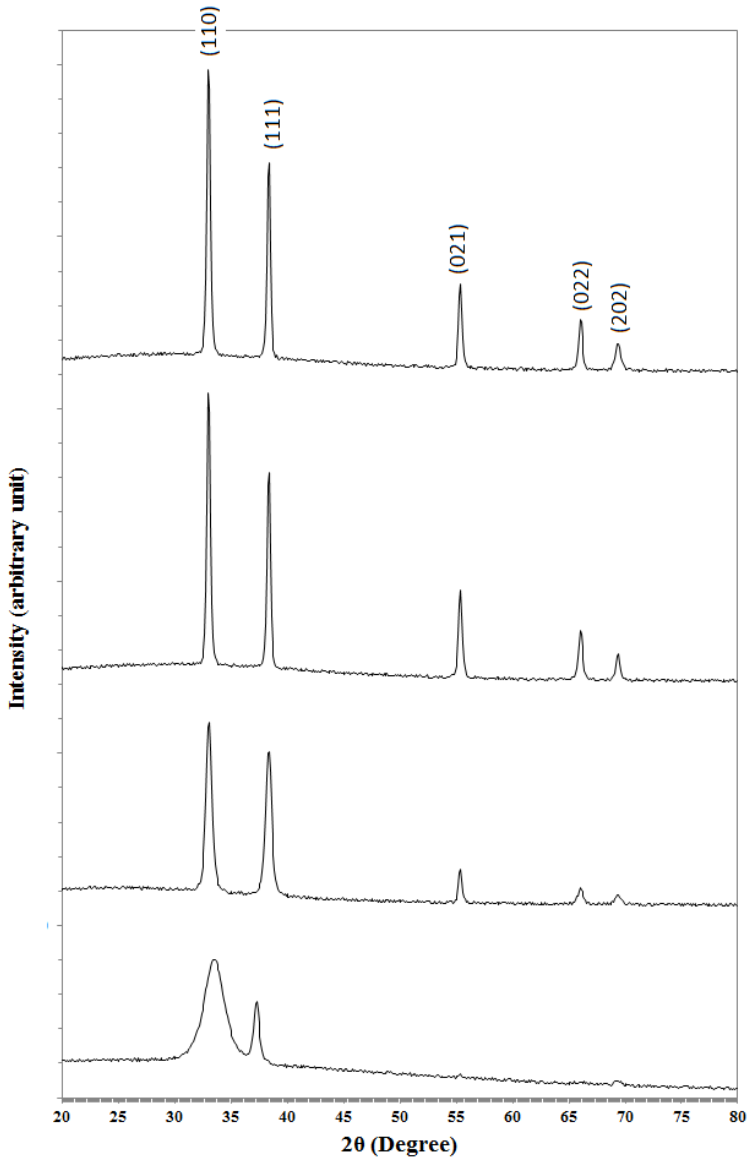

Fig. (3) The XRD patterns for MgO films doped with different concentrations of CuO

The carrier concentration (n_H) was increasing while the Hall mobility (μ_H) was decreased with increasing CuO content (as dopant) as well as with increasing annealing temperature. Such behaviors are attributed to the substitutional doping of CuO^{3+} in MgO structure creating one extra free carrier in the process. As the doping level is increased, more dopant atoms occupy lattice sites of Mg atoms

resulting in creating more charge carriers. Thus, the electrical conductivity of $(MgO)_{1-x}(CuO)_x$ samples was increased with increasing CuO content.

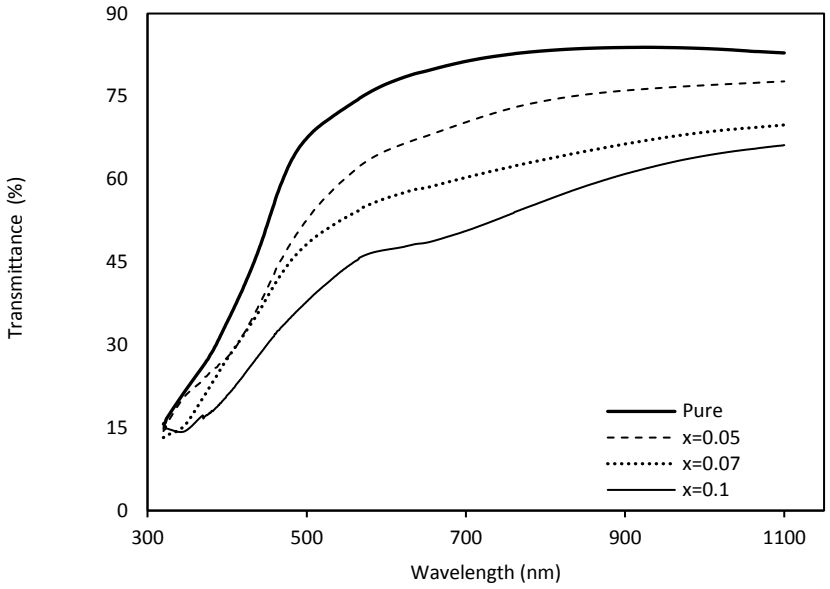

Fig. (4) Transmittance of $(MgO)_{1-x}(CuO)_x$ films as a function of wavelength at room temperature and different concentrations of CuO

Table (1) Hall effect parameters for $(MgO)_{1-x}(CuO)_x$ films prepared in this work

CuO content (wt.%)	Hall coefficient R_H (m^3/C) x10^7	Hall mobility μ_H ($cm^2/V.s$)
0 (pure MgO)	2.140	1700
0.1	1.34	1300
0.3	0.653	63.7
0.7	5.7	27.8
1 (pure CuO)	0.0328	280

The values of the optical energy gap (E_g) for $(MgO)_{1-x}(CuO)_x$ films were determined by Tauc equation to find the type of optical transition. This was done by plotting $(\alpha h\nu)^r$ versus photon energy ($h\nu$) and extrapolation of the linear part. It was found that the relation for r=2 yields linear dependence, which describes the allowed direct transition. The value of the optical energy gap was decreased from 3.25 to 2.90 eV with increasing CuO concentration. This is due to the increase in the density of localized states in E_g, which is shifted to lower values [19]. The values of E_g for different concentrations of CuO and annealing temperatures are listed in table (3).

Table (2) Measured carrier concentration and type of conductivity of the $(MgO)_{1-x}(CuO)_x$ films prepared in this work

CuO content (wt.%)	Carrier concentration n_H (cm^{-3}) x10^{11}	Type of conductivity
0 (pure MgO)	2.91	p-type
0.1	4.65	p-type
0.3	9.55	p-type
0.7	10.1	p-type
1 (pure CuO)	190	p-type

The absorption tails at energies smaller than the optical energy gap are called Urbach energy (E_u), which is evaluated by the plot of logarithmic value of absorption coefficient ($ln\ \alpha$) versus photon energy ($h\nu$) as shown in Fig. (5). The reciprocal of slope of the liner part gives the value of E_u. The Urbach energy gives information about the localized energy states. It is increased with increasing CuO concentration, which can be attributed to the production of new states in the energy gap. This may

explain the increase in the width of valence and conduction band tails that causes the increase in the value of E_u [20].

An interesting result from this work is the variation of E_u with E_g that can be seen from table (3). The coefficient β' (Tauc's slope) is obtained from the squared slope of the straight line. We observed from table (3) that β' is decreased with increasing CuO concentration. It is well known that β' is inversely proportional to the randomness of amorphous structure as well as to the width of the band tails [21]. So, larger β' value means smaller randomness.

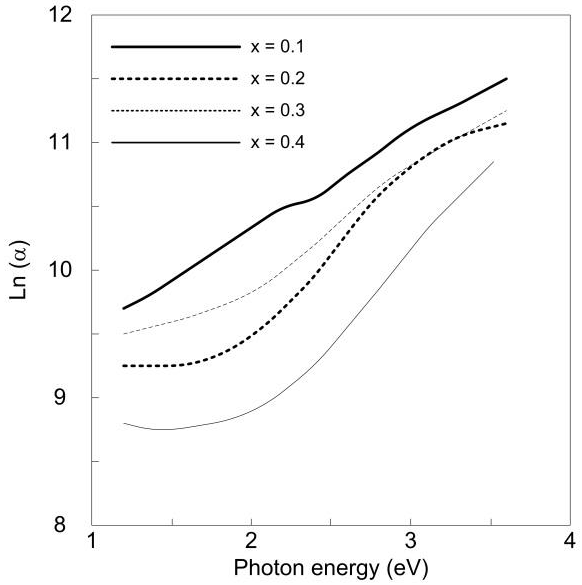

Fig. (5) Plot of ($ln\ \alpha$) versus photon energy (hv) for the $(MgO)_{1-x}(CuO)_x$ films prepared at room temperature and different concentrations (x) of CuO

Table (3) Optical results for the $(MgO)_{1-x}(CuO)_x$ films prepared in this work

CuO content (x)	E_g (eV)	E_u (eV)	β' (eV/cm^2) ×10^{21}
0 (pure MgO)	3.25	1.805804	9.314
0.05	3.20	2.310638	8.092
0.07	3.00	3.037853	7.364
0.1	2.90	4.218902	2.849

Figure (6) shows the variation of sensitivity to NO_2 gas of pure and CuO-doped MgO thin films prepared in this work with operation temperature in the range 25-300°C. The sensing measurements were carried out using 60 ppm NO_2 gas mixed with air at 3% concentration with bias voltage of 6V applied between the electrodes on the sample surface. The maximum sensitivity to NO_2 gas by pure MgO sensor was about 30% at 300°C, while the MgO film doped with 0.07 wt.% CuO showed reasonable enhancement in sensitivity to NO_2 gas at 300°C to reach 99.34%.

All results have shown that the sensitivity of MgO composite gas sensors to the oxidizing gas was greatly enhanced. This can be attributed to the nano-sized MgO particles on glass substrates as the amount of surface-adsorbed oxygen species was increased too [18,19]. Furthermore, it is well known that the conductivity of a semiconductor gas sensor is mainly determined by the presence of singly-charged oxygen vacancies [8] and the surface adsorbed oxygen species plays an important role during the sensing process [9,21].

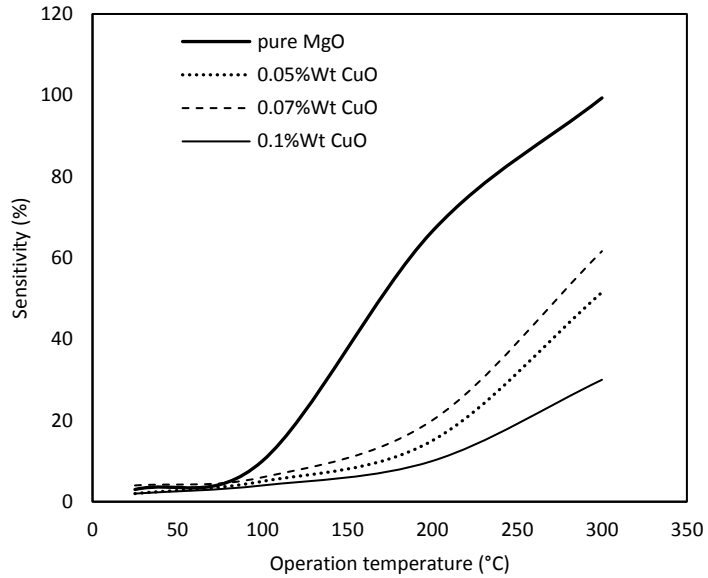

Fig. (6) Variation of sensitivity to NO_2 gas with operation temperature for pure and CuO-doped MgO thin film gas sensors fabricated in this work

The response and recovery times of the pure MgO film for 3% NO_2 gas and 10% NH_3:air gas mixing ratios were determined. The successive tests were performed at a bias voltage of 6V. Figures (7a) and (7b) indicate the response time and recovery time, respectively, of the pure and CuO-doped MgO thin film gas sensors. The response time was increasing and recovery time was decreasing with increasing CuO concentration. The shortest response time was 18 s for pure MgO film sample while the shortest recovery time was 43.2 s at 0.1 wt.% CuO concentration.

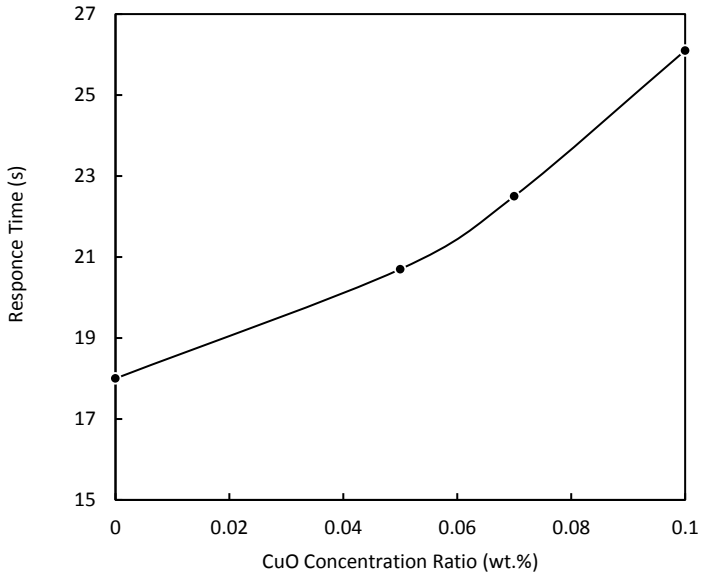

ISSN (print) 2958-8960 (online) xxxx-xxxx Printed in IRAQ

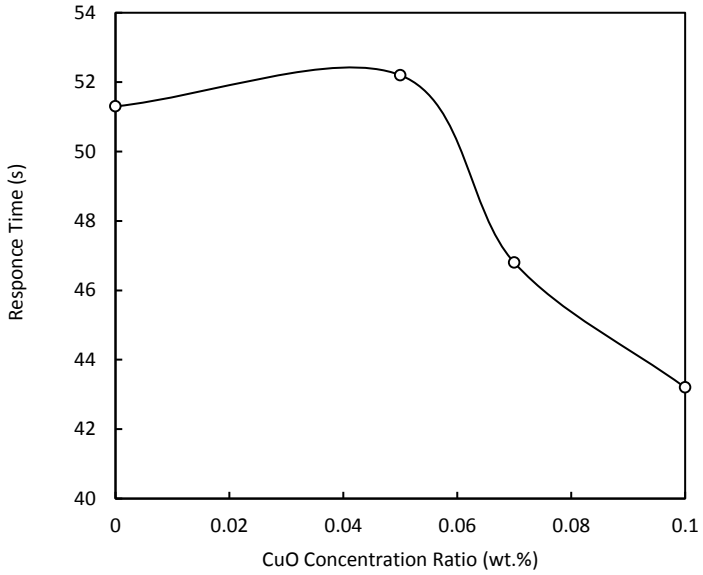

Fig. (7) Variation of response time (a) and recovery time (b) for pure and CuO-doped MgO thin film gas sensors fabricated in this work at optimum operating temperature (300°C)

4. Conclusions

Pure and doped magnesium oxide (MgO) thin films doped with different concentrations (0.05, 0.07, 0.1) wt.% of copper oxide (CuO) were deposited on glass substrates by pulsed-laser deposition technique to fabricate gas sensors. The prepared MgO:CuO nanostructures films are polycrystalline with tetragonal rutile phase for MgO and monoclinic phase for CuO. The transmittance and energy gap of all prepared samples were decreased while the absorption coefficient was increased with increasing CuO content. The effects of varying operation temperature of the fabricated gas sensors on sensor sensitivity and response time were studied and maximum sensitivity of about 99.34% was determined for pure MgO.

References

[1] C. Ristoscu and I. N. Mihailescu, “Effect of Pulse Laser Duration and Shape on PLD Thin Films Morphology and Structure BT - Lasers - Applications in Science and Industry,” Lasers - Appl. Sci. Ind., No. 3 (2011) 53–74.
[2] O.A. Hamadi, “Characteristics of CdO-Si Heterostructure Produced by Plasma-Induced Bonding Technique”, Proc. IMechE, Part L, J. Mater.: Design and Applications, 222 (2008) 65-71, DOI: 10.1243/14644207JMDA56.
[3] O.A. Hamadi, “Effect of Annealing on the Electrical Characteristics of CdO-Si Heterostructure Produced by Plasma-Induced Bonding Technique”, Iraqi J. Appl. Phys., 4(3) (2008) 34-37.
[4] A.A.K. Hadi and O.A. Hamadi, “Optoelectronic Characteristics of As-doped Silicon Photodetectors Produced by LID Technique”, Iraqi J. Appl. Phys. Lett., 1(2) (2008) 23-26.
[5] N. Tamaekong, C. Liewhiran and S. Phanichphant, “Synthesis of thermally spherical CuO nanoparticles,” J. Nanomater., vol. 2014 (2014) Article ID: 507978.
[6] O.A. Hammadi, “Photovoltaic Properties of Thermally-Grown Selenium-Doped Silicon Photodiodes for Infrared Detection Applications”, Photonic Sensors, 5(2) (2015) 152-158, DOI: 10.1007/s13320-015-0241-4
[7] O.A. Hammadi and N.E. Naji, “Electrical and Spectral Characterization of CdS/Si Heterojunction Prepared by Plasma-Induced Bonding”, Opt. Quant. Electron., 48(8) (2016) 375.
[8] K. Kaviyarasu, C. M. Magdalane, K. Anand, E. Manikandan and M. Maaza, “Molecular and Biomolecular Spectroscopy Synthesis and characterization studies of MgO:CuO nanocrystals by wet-chemical method”, Spectrochimica Acta Part A, 142 (2015) 405-409.
[9] I.E. Wachs, G. Deo, J.-M. Jehng, D. S. Kim, and H. Hu, “The Activity and Selectivity Properties of Supported Metal Oxide Catalysts During Oxidation Reactions”, Heterogen. Hydrocarbon Oxid., 638 (1996) 292-299.
[10] O.A. Hammadi, M.K. Khalaf, F.J. Kadhim, “Fabrication of UV Photodetector from Nickel Oxide Nanoparticles Deposited on Silicon Substrate by Closed-Field Unbalanced Dual Magnetron Sputtering Techniques”, Opt. Quantum Electron., 47(12) (2015) 3805-3813. DOI: 10.1007/s11082-015-0247-6
[11] O.A. Hammadi, M.K. Khalaf, F.J. Kadhim, “Fabrication and Characterization of UV Photodetectors Based on Silicon Nitride Nanostructures Prepared by Magnetron Sputtering”, Proc. IMechE, Part N, J. Nanoeng. Nanosys., 230(1) (2016) 32-36. DOI: 10.1177/1740349915610600
[12] S. Wang, F. Tristan, D. Minami, T. Fujimori, R. Cruz-Silva, M. Terrones, K. Takeuchi, K. Teshima, F. Rodríguez-Reinoso, M. Endo and K. Kaneko, “Activation routes for high surface area graphene monoliths from graphene oxide colloids”, Carbon, 76 (2014) 220-231.
[13] A.K. Balta, Ö. Ertek, N. Eker and İ. Okur, “MgO and ZnO Composite Thin Films Using the Spin Coating Method on Microscope Glasses”, Mater. Sci. Appl., 6(1) (2015) 40–47.

[14] O.A. Hammadi, M.K. Khalaf, F.J. Kadhim, "Silicon Nitride Nanostructures Prepared by Reactive Sputtering Using Closed-Field Unbalanced Dual Magnetrons", Proc. IMechE, Part L, J. Mater.: Design and Applications, 231(5) (2017) 479-487, DOI: 10.1177/1464420715601151.
[15] Y.R. Hathal, I.M. Ibrahim, F.T. Ibrahim and M.H. Ali, "Sensing Behavior of CuO:NiO/PS Nanoparticles", Austral. J. Basic Appl. Sci., 9(23) (2015) 682–688.
[16] M.Y.A. Ates, M.A. Yildirim, M. Kundakçi and M. Yildrim, "Investigation of Optical and Structural Properties of CdS Thin Films," Chinese J. Phys., 45(2) (2007) 135–141.
[17] M. Rashad, R. Amin, M.M. Hafiz and N. Valley, "Redshift in the optical band gap of amorphous nanostructure $Se_{80}Te_{20-x}Sn_x$ films", Chalcog. Lett., 9(12) (2015) 441–451.
[18] A.N. Naje, R.R. Ibraheem and F.T. Ibrahim, "Parametric Analysis of NO_2 Gas Sensor Based on Carbon Nanotubes", Photon. Sens., 6(2) (2016) 153-157.
[19] I.M. Ibrahim, S.I. Sharhan and F.T. Ibrahim, "Sensing behavior of CuO-doped ZnO/PS nanoparticles," Mater. Lett., 157(7) (2015) 57-62.
[20] K. Iijima, M. Goto, S. Enomoto, H. Kunugita, K. Ema, M. Tsukamoto, N. Ichikawa and H. Sakama, "Influence of oxygen vacancies on optical properties of anatase TiO_2 thin films," J. Lumin., 128(5-6) (2008) 911-913.
[21] M. Setvín, U. Aschauer, P. Scheiber, Y.-F. Li, W. Hou, M. Schmid, A. Selloni and U. Diebold, "Reaction of O_2 with subsurface oxygen vacancies on TiO2 anatase (101)", Science, 341(6149) (2013) 988-991.

 ISSN (print) 2958-8960 (online) xxxx-xxxx Printed in IRAQ